Talanta 111 (2013) 20–27

Contents lists available at SciVerse ScienceDirect

Talanta

journal homepage: www.elsevier.com/locate/talanta

Study on stability mechanism of immobilized pH gradient in isoelectric focusing via the Svensson–Tiselius differential equation and moving reaction boundary

Chen-Gang Guo, Si Li, Hou-Yu Wang, Dong Zhang, Guo-Qing Li, Jie Zhang, Liu-Yin Fan, Cheng-Xi Cao*

Key State Laboratory of Microbial Metabolism, School of Life Science and Biotechnology, Shanghai Jiao Tong University, Shanghai 200240, China

ARTICLE INFO

Article history:
Received 8 December 2012
Received in revised form
7 March 2013
Accepted 10 March 2013
Available online 16 March 2013

Keywords:
Immobilized pH gradient
Isoelectric focusing
Moving reaction boundary
Differential equation

ABSTRACT

An immobilized pH gradient (IPG) has strong power against instability (e.g., drifting and plateau) existing in classic isoelectric focusing (IEF). However, the relevant mechanism against the instability of pH gradient is still unclear. In this work, the theories of diffusional current and water products in IEF were developed based on the Svensson–Tiselius's differential equation and concept of moving reaction boundary (MRB). Two novel methods of pH gradient mobilization in IPG–IEF and non-IPG–IEF (opposite to IPG–IEF) were developed to unveil stability mechanism of IPG–IEF. The theoretical and experimental results indicated that (i) the drifting of pH gradient in non-IPG–IEF could be effectively controlled by IPG technique due to the existence of equal-fluxes of hydroxyl and hydrogen ions in the IPG–IEF system, (ii) there existed high diffusional current in non-IPG–IEF because of the existence of free carrier ampholyte (CA), but weak current in the IPG–IEF due to the immobilization of CA species in gel matrix, and (iii) the high diffusional current resulted in a great amount of water formation in neutral zone of pH gradient that led to distinct plateau in non-IPG–IEF, conversely the weak diffusional current caused little of water formation and weak plateau of pH gradient in IPG–IEF. These studies have considerable significance to the understanding of mechanism and development of protein IEF separation technique.

1. Introduction

Isoelectric focusing (IEF) is a powerful technique separating different proteins in line with their pIs in a pH gradient [1]. In 1961–1962, Svensson [2,3] advanced the classic theory of IEF and indicated the key role of carrier ampholyte (CA) in formation of pH gradient in IEF. According to the classic theory, Vesterberg [4,5] in 1967–1969 successfully synthesized the material of CA, resulting in the actual uses of gel–slab IEF in biological research. In 1970, O'Farrell [6] firstly constructed the two-dimensional gel electrophoresis (2DE) system, in which IEF was applied as the first dimensional separation technique of complex protein sample. During the last two decades, 2DE has become a standard separation method in proteomics [7,8].

However, the classic IEF suffered from instability of pH gradient, including drifting and plateau of pH gradient as well as pH gradient mobilization, which could not be explained by Svennson's theory [1–3]. To explore the mechanism of instability, numerous hypotheses were developed, such as (i) isotachophoretic (ITP) migration of ampholytes [9–12], (ii) CO_2 adsorption at the cathodic gel end [13], (iii) focusing and formation of pure water zone within pH gradient [14,15], (iv) selective deficiency and interaction of ampholyte [13,16], (v) progressive gain or loss of charged ligand by CA [13], and (vi) unbalance migration between hydrogen and hydroxyl ions [17,18]. Nevertheless, the instability is still present in a classic IEF.

To address the issues of drifting and plateau of pH gradients, Righttti et al. in 1980s advanced the important concept of immobilized pH gradient (IPG) and successfully synthesized the IPG gel strip for both IEF run [19–22] and 2DE separation [23,24]. Currently, the commercial IPG gel strip is available from both GE and Bio-Rad companies. The IPG–IEF technique could greatly improve the stability of pH gradient. Recently, IPG technique was further used in capillary IEF [25,26], microchip IEF [27] and prefractionation of protein and peptide [28]. However, the relevant physico-chemical mechanism is indeed complex and still unclear, as will be revealed in this work.

The theories of moving reaction boundary (MRB) [29,30] suggest a pathway to unveil the exact mechanism of stable pH gradient in IPG–IEF. The MRB concept was developed from the important ideas of moving reactive front (MRF) advanced by Deman [31,32] and stationary neutralization boundary by Pospichal [33,34]. Based on the above-mentioned concept, our laboratory along with Liang et al. [35,36] have evolved the physico-chemicalchemical model and theory of IEF. Furthermore, we qualitatively explained the mechanism, why there was a quasi-stability of pH gradient in a classic IEF [30,37], and gave the semi-quantitative explanation on pH gradient instabilities [30] and Hjerten's mobilization [30,38]. These results

* Corresponding author. Tel./fax: +86 21 34205820.
E-mail address: cxcao@sjtu.edu.cn (C.-X. Cao).

0039-9140/$ - see front matter Crown Copyright © 2013 Published by Elsevier B.V. All rights reserved.
http://dx.doi.org/10.1016/j.talanta.2013.03.026

[29,30,35–38] indicate that the two necessary conditions to a stable pH gradient in IEF are (i) the gain of equal-fluxes of hydrogen in the anolyte and hydroxyl ions in the catholyte and (ii) the effective weakening of water production.

The main purposes in our studies are further to explore the stability mechanism of IPG–IEF. For this purpose, we develop the relevant judgement expressions for fluxes comparing of hydrogen and hydroxyl ions in the IPG–IEF system, define the concept of relative diffusional current for description of water production in IEF, design a novel IEF method for the relevant study, and unveil the exact mechanism of controlling pH gradient drifting and plateau in IPG–IEF via the developed theory.

2. Materials and methods

2.1. Chemicals

Readystrip™ IPG strips (7 cm in length, pH 3–10), Bio-Lyte pH 3–10 ampholytes and IEF standard proteins (p*I* 4.45–9.6), including nine kinds of model proteins of phycocyanin, β-lactoglobulin B, bovine and human carbonic anhydrase, equine myoglobin, human hemoglobin A and C, lentil lectin, and cytochrome C), along with mineoil, were purchased from Bio-Rad Laboratories (Mississauga, Canada), Milli-Q grade water was purified to 18.2 MΩ cm^{-1}. Ployacrylamide, Bis-acrylamide, ammonium persulfate and methylcellulose (MC) were purchased from Sigma. All other chemicals were gained from Sigma and directly used without further purification.

2.2. Instruments

All of IEF runs, including IPG–IEF and non-IPG–IEF, were performed with a Multiphor II Electrophoresis Unit (LKB Co., Sweden) and a 2197 power supply (LKB Co., Sweden). A circle water cooling device (Ningbo XinYi Instrument Ltd., Ningbo, China) was used for controlling temperature of the cooling plate in the Multiphor II Electrophoresis Unit. A 7-cm long IEF tray originally used in the PROTEAN IEF System (Bio-Rad Laboratories Headquarters, USA) was applied for the experiments of IPG–IEF and non-IPG–IEF. A PAGE apparatus (Mini Protean Tetra Cell, Bio-Rad Laboratories Headquarters) was supplied for the synthesis of non-IPG gel strip. A digital camera was used for imaging (Olympus Co., Japan). A digital multimeter (DT9205A^{+}, Zhangzhou Weihua Electronic Co., Ltd., Fujian, China) was in series with the Multiphor II Electrophoresis Unit and the 2197 power supply for the monitoring of the current during a IPG–IEF or non-IPG–IEF run.

2.3. Experimental procedures

2.3.1. IPG–IEF

Rehydration: The rehydration of IPG gel strip was handled in a rehydration tray according to manufacturer's introduction. The rehydration solution (total volume150 μl) for each IPG gel strip was composed of 30 μl glycerol (20%, v/v), 1.9 μl 40% carrier ampholyte (0.5%, v/v), 2 μl IEF standard protein sample, and 116 μl ultrapure water. After 10 min of rehydration, the strip was covered with about 1 mL mineral oil added dropwise. The rehydration was set overnight.

Run of IPG–IEF: The rehydrated IPG strips were taken from the rehydration tray and taken out from the mineral oil. Then the strips were immediately placed into the focusing tray slot (Fig. 1A). 1 mL mineral oil was added into the tray slot preventing water evaporation from the strips. The IPG–IEF run was carried out at 100 V for 30 min, followed by a stepwise voltage from 200 V to 800 V (1 h and 100 V as interval time and voltage, respectively). Finally the constant voltage of 800 V was kept until the end of IEF run. The cooling temperature was set at 15 °C.

Imaging of protein zones in IPG–IEF: The electrophoregram of chromoprotein zones during an IPG–IEF run was photographed every 60 min from 240 min to 780 min by an Olympus digital camera. One did not record the electrophoregram before 240 min as the zones were not focused well within 240 min IPG–IEF run.

Detection of electric current: The electric current was recorded every 5 min during an IPG–IEF run via a digital multimeter was in series with a LKB IEF system (the Multiphor II Electrophoresis Unit and the 2197 power supply mentioned above) and a Bio-Rad 7-cm in length IEF focusing tray. Then the curve of current versus the run time of IEF was obtained by the software of Origin 8.0.

2.3.2. Non-IPG–IEF

Preparation of non-IPG–IEF gel: A thin PAG gel (5%T, 3%C) was prepared for the relevant study in line with the procedure in Ref. [39]. Briefly, the thin PAG layer was synthesized based on a Bio-Rad PAGE apparatus (Mini Protean Tetra Cell). After polymerization, the thin PAG gel on a glass was removed from the frame of PAGE apparatus and dried at 25 °C in a dust-free oven. Then, the dried thin PAG gel was cut and made into non-IPG gel strip with 3 mm in width and 7 cm in length. The dried non-IPG gel strip was placed in the slot of 7-cm long focusing tray (Bio-Rad Laboratories) for rehydration in situ. The size of rehydrated non-IPG gel strip was designed to be the same as that (3 mm × 1.18 mm (including 1 mm IPG gel layer and 0.18 mm backing film)) of IPG gel strip for the following comparative experiments of diffusional currents between the IPG–IEF and non-IPG–IEF system (Section 3.2.4). The rehydration solution (150 μl for each gel strip) was composed of 30 μl 20% (v/v) glycerol, 7.5 μl 2% (v/v) carrier ampholyte (pH 3–10),

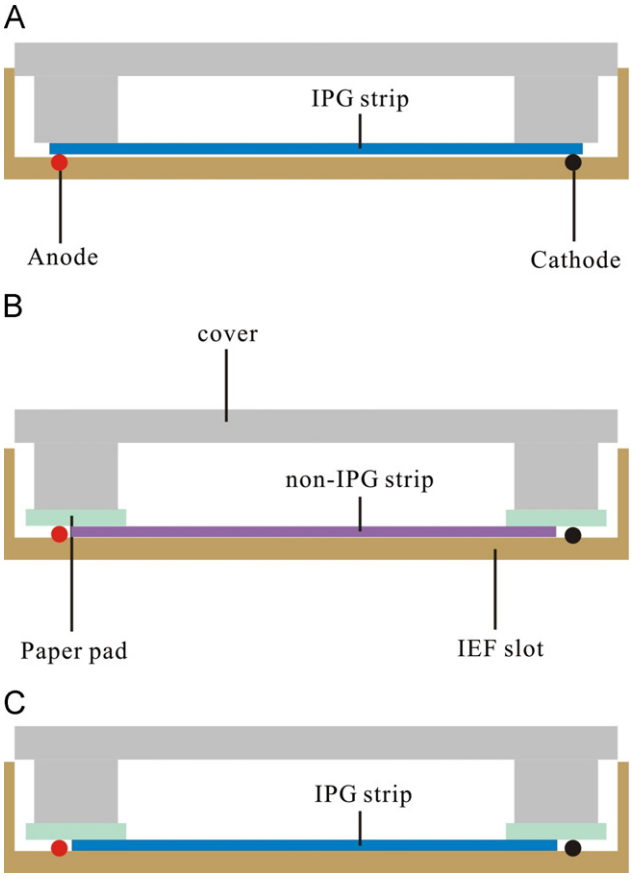

Fig. 1. Schematic diagrams of IPG–IEF (A), non-IPG–IEF (B) and IPG–IEF with paper pads (C).

2 μl IEF standard protein sample, and 110.5 μl ultrapure water, being the same as the composition of rehydrattion solution of IPG gel strip except for the content of carrier ampholyte. After 10 min of rehydration, the gel strips were covered with about 1 mL mineral oil and the rehydration was performed overnight.

Run of non-IPG–IEF: For a non-IPG–IEF run, 80 mM H_2SO_4 and 200 mM NaOH were used as the anolyte and catholyte, respectively. Prior to a non-IPG-IEF run, the filter paper pads were individually immersed into the anolyte and catholyte overnight. Next day, the immersed paper pads bridged between the non-IPG gel strip and the electrodes (Fig. 1B). The following steps and conditions for non-IPG–IEF were the same as those of IPG–IEF mentioned in Section 2.3.1.

Finally, we imaged every 60 min from 300 min to 840 min and recorded the electric current every 5 mins during a non-IPG–IEF run. The other procedures were the same as those of IPG–IEF experiments mentioned in Section 2.3.1.

2.3.3. IPG–IEF with electrode paper pads

The electrode paper pads were individually immersed in 80 mM H_2SO_4 and 200 mM NaOH overnight. Prior to IEF run, the rehydrated IPG gel strip was set between the anode and the cathode (Fig. 1C). The anode paper pad (with 80 mM H_2SO_4) or the cathode pad (with 200 mM NaOH) bridged the gel strip and the electrodes respectively. And then 1 mL mineral oil was dropped into the slot of focusing tray preventing IPG gel strip water evaporation. The other procedure, including the rehydration, IEF run condition and imaging of focused standard protein zones, was the same as that of IPG–IEF experiments in Section 2.3.1.

2.3.4. IPG–IEF with Hjerten's mobilization

The procedure of IEF with Hjerten's mobilization was similar to that reported in Ref. [38], but with some modification. In this study, one used sulfuric acid (80 mM) as the anolyte and sodium hydroxide (200 mM) as the catholyte. Anodic and cathodic salt-gradient solutions were prepared. The anodic salt gradient solutions contained 20 mM H_2SO_4+50, 100, 150 and 200 mM Na_2SO_4 (Table 1), and the cathodic ones had 200 mM NaOH+50, 100, 150 and 200 mM Na_2SO_4 (Table 2). The anode and cathode paper pads were respectively immersed into the anodic and cathodic salt gradient solutions (Tables 1 and 2) before used. Rehydration solution recipe in the experiment was the same as that of IPG–IEF (Sections 2.3.1 and 2.3.3).

IPG–IEF with Hjerten's mobilization was initially carried out using the electrode paper pads with 80 mM H_2SO_4 and 200 mM NaOH (Section 2.3.3). The run was paused when the focusing reached its steady-state (8 h run of IPG–IEF). Then, the anode (80 mM sulfuric acid) and cathode (200 mM NaOH) paper pads were respectively displaced with those having the anodic and cathodic salt gradient solutions. After that, the IPG-–IEF run again. The electrophoregram of IPG–IEF run from 9 h to 68 h (12 h as imaging interval time) was recorded by a digital camera.

3. Results and discussion

3.1. Theoretical results

3.1.1. Judgment expressions for IPG–IEF

In order to compare the fluxes of hydrogen and hydroxyl ions in an IPG–IEF system, it is necessary to define the absolute expression [29,30]

$$R_{\mathrm{abs}} = m_{+}^{\alpha}\ c_{+}^{\alpha}\ \kappa^{\beta} - m_{-}^{\beta}\ c_{-}^{\beta}\ \kappa^{\alpha} \tag{1}$$

where R is the symbol of judgment expression, the subscript "abs" means the absolute one, κ is the conductivity of a solution or phase (S/m); m is the ionic mobility ($m^2\ s^{-1}\ V^{-1}$); c is the equivalent concentration (equiv./l), the subscripts, "+" and "−", imply the positive and negative reacting ions, such as hydrogen and hydroxyl ions, respectively, and the superscripts, "α" and "β", mean phase α and phase β, respectively. For a pure acid–base system used in IEF, one has the following relative judgement expressions for the comparison of hydrogen and hydroxyl ion fluxes [29,30]

$$R_{\mathrm{r}} = \frac{m_{H^+}^{\alpha}\ \lambda_{OH^-}^{\beta}}{m_{OH^-}^{\beta}\ \lambda_{H^+}^{\alpha}} - 1 (\mathrm{for} R_{\mathrm{abs}} \geq 0) \tag{2a}$$

$$R_{\mathrm{r}} = 1 - \frac{m_{OH^-}^{\beta}\ \lambda_{H^+}^{\alpha}}{m_{H^+}^{\alpha}\ \lambda_{OH^-}^{\beta}} (\mathrm{for} R_{\mathrm{abs}} < 0) \tag{2b}$$

where the subscript "r" means the relative judgement expressions, λ is the ionic equivalent conductivity in a pure electrolytes. It is defined as [40,41]

$$\lambda_i = m_i F \tag{3}$$

Suprisingly, when inserting Eq. (3) into Eqs. (2a) and (2b), one get Eqs. (4a) and (4b), respectively:

$$R_{\mathrm{r}} = 0 (\mathrm{for} R_{\mathrm{abs}} \geq 0) \tag{4a}$$

$$R_{\mathrm{r}} = 0 (\mathrm{for} R_{\mathrm{abs}} < 0) \tag{4b}$$

Table 1
R_r values and significances for the salt gradient drifting experiment by adding salt in the anolyte.

Number[a]	Anolyte	Catholyte	R_r	Prediction	Experiment in Fig. 5
1	80 mM H_2SO_4+50 mM Na_2SO_4	200 mM NaOH	−0.240	4th anodic drifting	4th anodic drifting
2	80 mM H_2SO_4+100 mM Na_2SO_4	200 mM NaOH	−0.809	3rd anodic drifting	3rd anodic drifting
3	80 mM H_2SO_4+150 mM Na_2SO_4	200 mM NaOH	−1.692	2nd anodic drifting	2nd anodic drifting
4	80 mM H_2SO_4+200 mM Na_2SO_4	200 mM NaOH	−2.976	1st anodic drifting	1st anodic drifting

[a] The numbers herein correspond with Panels A–D in Fig. 5.

Table 2
R_r values and significances for the salt gradient drifting experiment by adding salt in the catholyte.

No.[a]	Anolyte	Catholyte	R_r	Prediction	Experiment in Fig. 6
1	80 mM H_2SO_4	200 mM NaOH+50 mM Na_2SO_4	0.479	4th cathodic drifting	4th cathodic drifting
2	80 mM H_2SO_4	200 mM NaOH+100 mM Na_2SO_4	0.879	3rd cathodic drifting	3rd cathodic drifting
3	80 mM H_2SO_4	200 mM NaOH+150 mM Na_2SO_4	1.320	2nd cathodic drifting	2nd cathodic drifting
4	80 mM H_2SO_4	200 mM NaOH+200 mM Na_2SO_4	1.803	1st cathodic drifting	1st cathodic drifting

[a] The numbers herein correspond with Panels A–D in Fig. 6.

The significance of $R_r=0$ is that the flux of hydrogen ion is equal to that of hydroxyl ion, indicating no cathodic or anodic drifting of pH gradient in the IPG–IEF system.

At present, it is very difficult to calculate the exact experimental value of R_r in IPG–IEF because one cannot obtain the specific conductivities of the anodic and cathodic ends of IPG gel strip, unlike conductivity of anodic and cathodic solutions in a classic IEF easily obtained via a conductance-meter [29,30]. Although the direct experimental value of R_r in IPG–IEF cannot be obtained, we may get the indirect value of R_r in IPG–IEF (being close to zero) via the analogical experiments in Section 3.2.

3.1.2. Currents in IEF

In the initial stage of the IEF system, the electromigration current (EMC) of ion i ($I_{EMC,i}$) is given as [40,41]

$$I_{EMC,i}=\frac{c_i}{1000}v_iAF \tag{5}$$

where A is the cross-sectional area of electrophoretic tube. The total current is originated from the electromigrations of various CA species, hydrogen and hydroxyl ions (omission of the current from protein electromigration). Thus, the total EMC at an initial stage of IEF ($I_{EMC,initial}$) is [40,41]

$$I_{EMC,initial}=(\sum c_iv_i+c_{H^+}v_{H^+}+c_{OH^-}v_{OH^-})\frac{AF}{1000} \tag{6}$$

where the subscript "initial" means the initial stage of IEF, the velocity of CA species is $v_i=m_iE$[29,30].

At a steady-state of IEF, CA species are focused at their pI positions, indicating the net zero mobilities of CA species (viz., $mi=0$). However, the hydrogen and hydroxyl ions are still present at the steady-state of IEF. Thus, Eq. (11) becomes

$$I_{EMC,SS}=(c_{H^+}v_{H^+}+c_{OH^-}v_{OH^-})\frac{AF}{1000} \tag{7}$$

where the subscript of "SS" indicates the steady-state of IEF. Assuming uniform conductivity and cross-sectional area, the distribution of CA_i can be described by Svensson–Tiselius' differential Eqs. (1–3),

$$\frac{C_im_iI}{A\kappa}=D_i\frac{dC_i}{dx_i} \tag{8}$$

where, C_i is the molar concentration (mol/L), D_i is the diffusion coefficient of the ion constituent, and dC_i/dx_i is the concentration gradient of focused CA_i. Eq. (8) implies that the electric mass flow of CA_i per-second and cross-sectional area is equal to the diffusional mass flow. If the conductance, diffusional coefficient and pH gradient are constant in the IEF system, then the analytic solution concentration of equations (8) for CA_i can be expressed as [1–3]

$$C_i=C_{0,i}\exp\left(E\frac{p_ix_i^2}{2D_i}\right) \tag{9}$$

where x is the coordinate for CA_i along the direction of current. Eq. (9) describes a Gaussian's concentration distribution (Supplementary Material Fig. S1) of CA_i focused at steady-state. In Fig. S1A, the consequence of diffusion-electromigration is that CA_i necessarily extends to or through the concentration maximum of the adjacent CA species (e.g., CA_{i-1} and CA_{i+1}). Fig. S1B reveals the steady-state of IEF at which the diffusion fluxes of CA_i are equal to the electromigration fluxes. Evidently, the diffusion of CA_i leads to electromigration of CA_i species from its adjacent species of CA_{i-1} and CA_{i+1}, indicating the formation of diffusional current originated from the CA_i diffusion. Thus, Eq. (8) can be expressed as

$$c_im_iE\frac{AF}{1000}=D_i\frac{dC_i}{dx_i}\frac{AF}{1000} \tag{10}$$

Eq. (10) can be defined as the diffusional current ($I_{DC,SS}$) of CA_i at steady-state of IEF. Hence, we have

$$I_{DC,SS}=c_im_iE\frac{AF}{1000}=D_i\frac{dC_i}{dx_i}\frac{AF}{1000} \tag{11}$$

Evidently, the total current ($I_{T,SS}$) at steady-state of IEF is

$$I_{T,SS}=I_{EMC,SS}+I_{DC,SS} \tag{12}$$

Inserting Eqs. (6) and (11) into Eq. (12), one gets

$$I_{T,SS,non\text{-}IPG}=\left(c_{H^+}v_{H^+}+c_{OH^-}v_{OH^-}+D_i\frac{dC_i}{dx_i}\right)\frac{AF}{1000} \tag{13}$$

where, the subscript "non-IPG" after the current of "I" indicates a non-IPG–IEF system, the subscript of "IPG" after the current of "I" implies an IPG–IEF system. Eq. (13) has validity for the total current in a non-IPG–IEF. However, for an IPG–IEF, the diffusional constant is close to zero due to the bonding of CA species to gel matrix. Evidently, for an IPG–IEF, Eq. (13) is written as

$$I_{T,SS,IPG}=(c_{H^+}v_{H^+}+c_{OH^-}v_{OH^-})\frac{AF}{1000} \tag{14}$$

3.1.3. Product of water in IEF at steady-state

In 1975, Baumann et al. [14] recognized the focusing and formation of pure water zone within pH gradient. In 2005, Li et al. [39] demonstrated the chemical reaction product in a MRB system, and defined product equivalent number of electromigration reaction in unit-time in a MRB system (R_{rate},equiv./s).

$$R_{rate}=I\frac{m_{OH^-}^{\beta}\kappa^{\alpha}-m_{H^+}^{\alpha}\kappa^{\beta}}{\kappa^{\alpha}\kappa^{\beta}}\frac{c_{H^+}^{\alpha}c_{OH^-}^{\beta}}{c_{H^+}^{\alpha}-c_{OH^-}^{\beta}} \tag{15}$$

Clearly, the combination of Eqs. (13) and (15) produces

$$R_{rate,SS,non\text{-}IPG}=I_{T,SS,non\text{-}IPG}\frac{1000}{AF}\frac{m_{OH^-}^{\beta}\kappa^{\alpha}-m_{H^+}^{\alpha}\kappa^{\beta}}{\kappa^{\alpha}\kappa^{\beta}}\frac{c_{H^+}^{\alpha}c_{OH^-}^{\beta}}{c_{H^+}^{\alpha}-c_{OH^-}^{\beta}} \tag{16}$$

which has validity for the formation of water in a non-IPG–IEF system. Inserting Eq. (14) into Eq. (15), one gets

$$R_{rate,SS,IPG}=I_{T,SS,IPG}\frac{1000}{AF}\frac{m_{OH^-}^{\beta}\kappa^{\alpha}-m_{H^+}^{\alpha}\kappa^{\beta}}{\kappa^{\alpha}\kappa^{\beta}}\frac{c_{H^+}^{\alpha}c_{OH^-}^{\beta}}{c_{H^+}^{\alpha}-c_{OH^-}^{\beta}} \tag{17}$$

Eq. (17) has validity for the product of water in an IPG–IEF system.

3.2. Experimental results

3.2.1. Comparison of stability in IPG–IEF and non-IPG–IEF

Fig. 2 showed the experimental results of IPG–IEF. As can be seen, the chromoprotein bands (blue phycocynin, brown Hb and Mb, and bright red cytochrome C) still were obscure within 360 min of IEF, suggesting an incompleted focusing. After 360 min of IEF run, it was observed that the chromoprotein bands became clearer and straighter without distinct drifting and/or plateau of pH gradient and their positions were almost constant until 780 min, implying high stability pH gradient existing in the IPG–IEF from 360 min to 780 min. The experiments (Supplementary Material Fig. S2) demonstrated the similar results. Therefore, IPG–IEF technique can overcome the pH gradient drifting and plateau phenomenon existing in non-IPG–IEF by immobilization of pH gradient.

Fig. 3 showed the experimental results of non-IPG–IEF. In Fig. 3, the blue phycocynin moves toward the anode obviously (2.87 mm) if the IEF run in 600 min, while brown protein Hb/Mb has rapid cathodic migration (3.28 mm), and the bright red cytochrome C also has significant drafting. All of these results revealed the imcomplete IEF for the colorful proteins if the focusing was set within about 600 min. During the IEF run of 600–840 min, the blue band held a slight anodic movement (1.23 mm) and the bright red band had

almost no movement, indicating no obvious anodic or cathodic pH gradient drifting during the long-term run of IEF. However, the brown bands of Mb (pI 7.0) and Hb (pI 7.1) obviously moved toward the cathode (1.33 mm). The cathodic movement of Mb/Hb, coupled with the quite constant positions of Phycocynin and cytochrome C during 600–840 min run, showed the apparent plateau of pH gradient, which also existed in a long-term non-IPG–IEF. The experiments (Supplementary Material Fig. S3) proved the similar plateau of pH gradient occurring in non-IPG–IEF.

From the comparison of experiments in Figs. 2 and 3, one could conclude that there were no obvious anodic or cathodic drifting and plateau of pH gradient after the steady-state (see the discussion below) in the long-time IPG–IEF run; whereas there still existed a clear plateau of pH gradient after the steady-state (about 600 min run) in the non-IPG–IEF.

3.2.2. Mechanism of weak pH gradient drifting in IPG–IEF

As revealed in the previous works [29,30,35–38], two necessary conditions for stable IEF run (viz., no cathodic or anodic drifting and plateau of pH gradient) wereas follows: (i) the R_r value was equal or close to zero, implying equal or quasi-equal fluxes of hydrogen and hydroxyl ions in IEF; and (ii) low produce rate of water formation, viz., low current intensity under the given voltage, at steady-state of IEF (Eqs. (16) and (17)). The first condition existed in a run of IPG–IEF, which had been theoretically unveiled in Eqs. (4a) and (4b). However, it was impossible to compute the exact R_r value in IPG–IEF since the specific conductivities of the anodic and cathodic ends could not be detected currently, unlike the easy measurement of conductivity of both anodic and cathodic solutions used in the classic IEF [30,35–38]. Though one could not directly calculate an experimental R_r value of IPG–IEF, an indirect experimental R_r value of IPG–IEF might be obtained via the analogical experiments as shown below.

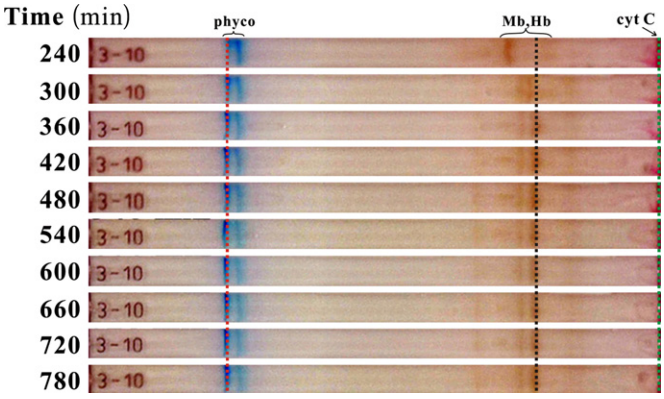

Fig. 2. Electrophoregrams of standard proteins focused in IPG–IEF under different running time. Experimental conditions: Bio-Rad linear IPG gel strips (pH 3–10), IEF run at 100 V for 30 min, stepwise voltage from 200 V to 800 V (1 h and 100 V as interval time and voltage, respectively), less than 50 μA/strip all the time, and 15 °C cooling. (phyco: phycocinin, Mb: equine myoglobin, Hb: human hemoglobin, and cyt C: cytochrome C).

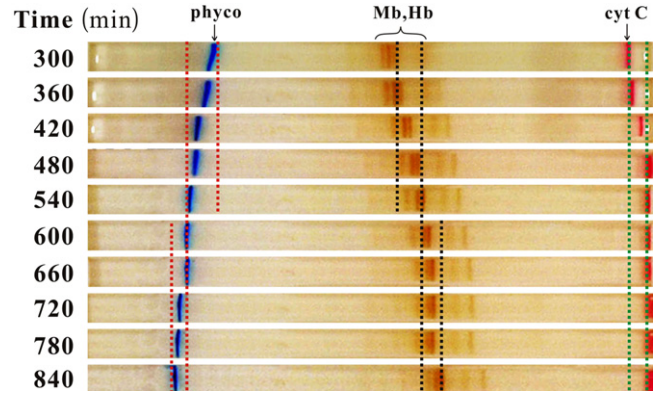

Fig. 3. Electrophoregrams of standard proteins focused in non-IPG–IEF under different running time. Experimental conditions: 80 mmol H_2SO_4 as the anolyte and 200 mmol NaOH as the catholyte, non-IPG gel strips (pH 3–10). The other conditions were the same as those in Fig. 2. (phyco: phycocinin, Mb: equine myoglobin, Hb: human hemoglobin, and cyt C: cytochrome C). (For interpretation of the references to color in this figure, the reader is referred to the web version of this article.)

It has been demonstrated in the previous works [29,30,35–38] that if there was $R_r \cong 0$, no cathodic or anodic drifting occurred in an IEF; conversely if there was no pH gradient drifting in an IEF, the R_r value ought to be close or equal to zero. To obtain an indirect experimental R_r value in Fig. 2, we further performed the analogical experiments of IPG–IEF runs with and without electrode paper pads. Fig. 4 presents the relevant experiments. In Fig. 4A, the experimental conditions are the same as these in Fig. 2 except for the long-term running time. In Fig. 4B, the conditions were the same as those in Fig. 4A except for the electrode paper pads. The anodic paper pad contained 80 mM H_2SO_4 and the cathodic pad had 200 mM NaOH. The R_r value calculated with Eq. (2a) for the electrode pad pairs was 0.082, being near zero [30,35–38].

The experiments in Fig. 4 reveal (i) that positions of the blue and brown bands are almost constant from 8 h to 68 h, indicating no drifting of pH gradient in Panel A, (ii) that the bands do not show any drifting even if the run lasted up to 68 h (Panel B), and (iii) that the bands in Panel A as a whole migrate slightly toward the cathode in contrast to these in Panel B. This just accounts for the correctness of experimental prediction of R_r value (0.082) in the electrolyte pairs of 80 mM H_2SO_4 and 200 mM NaOH [29,30,35–38]. The analogical experiments in Fig. 4 indicates that the R_r value of IPG–IEF without electrode paper pad pairs is very close to that of non-IPG–IEF with paper pad pairs (viz., $R_r = 0.082$), proving the validity of Eq. (4a).

Conversely, if the R_r value was obviously higher than zero, there was a clear cathodic drifting or mobilization of pH gradient; otherwise there was an evident anodic drifting or mobilization. The theoretical conclusion had been demonstrated by the experimental results cited from numerous references (Table S2 in [30]) and the recent experiments on pH gradient mobilization in a classic IEF [38]. The experiments given in Section 3.2.3 further manifest that even in an IPG–IEF, there was a clear cathodic drifting or mobilization of pH

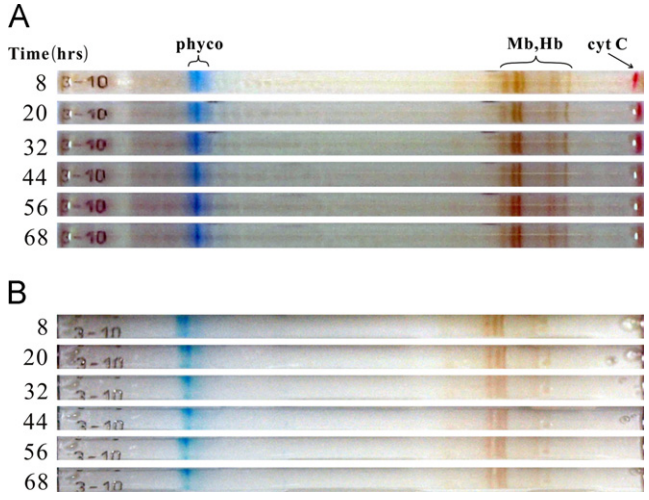

Fig. 4. Electrophoregrams of standard proteins focused in (A) IPG–IEF system with anodic paper pad of 80 mM H_2SO_4 and cathodic paper pad of 200 mM NaOH and (B) IPG–IEF system without paper pads. The other conditions were the same as those in Fig. 2. (Phyco: phycocinin, Mb: equine myoglobin, Hb: human hemoglobin, cyt C: cytochrome C). (For interpretation of the references to color in this figure, the reader is referred to the web version of this article.)

gradient if the R_r value was obviously greater than zero; on the contrary there was an evident anodic drifting or mobilization if greatly less than zero. The experimental results in Section 3.2.3 present the opposite proofs to indirectly demonstrate the validity of Eqs. (4a) and (4b).

3.2.3. *Mobilization of pH gradient in IPG–IEF*

A series of experiments on the pH gradient mobilization or drifting in IPG–IEF were performed by controlled hydrogen and hydroxyl ionic fluxes. Table 1 shows the R_r values for the systems of 80 mM H_2SO_4 with 50–200 mM Na_2SO_4 and 200 mM NaOH, and their significance was given in Section 3.1.1. The R_r values for numbers 1, 2, 3, and4 in Table 1 are −0.240, −0.809, −1.692, and −2.976 respectively, indicating the anodic mobilization or driftingof pH gradient [30,38]. Table 2 presents that the R_r values for the systems of 80 mM H_2SO_4 and 200 mM NaOH with 50–200 mM Na_2SO_4 were 0.479, 0.879, 1.320 and 1.803 respectively, implying the cathodic mobilization or drifting. The higher R_r value was, the more serious pH gradient instability was. The experiments in Tables 1 and 2 clearly demonstrat two predictions. The experiments given below further validated the predictions.

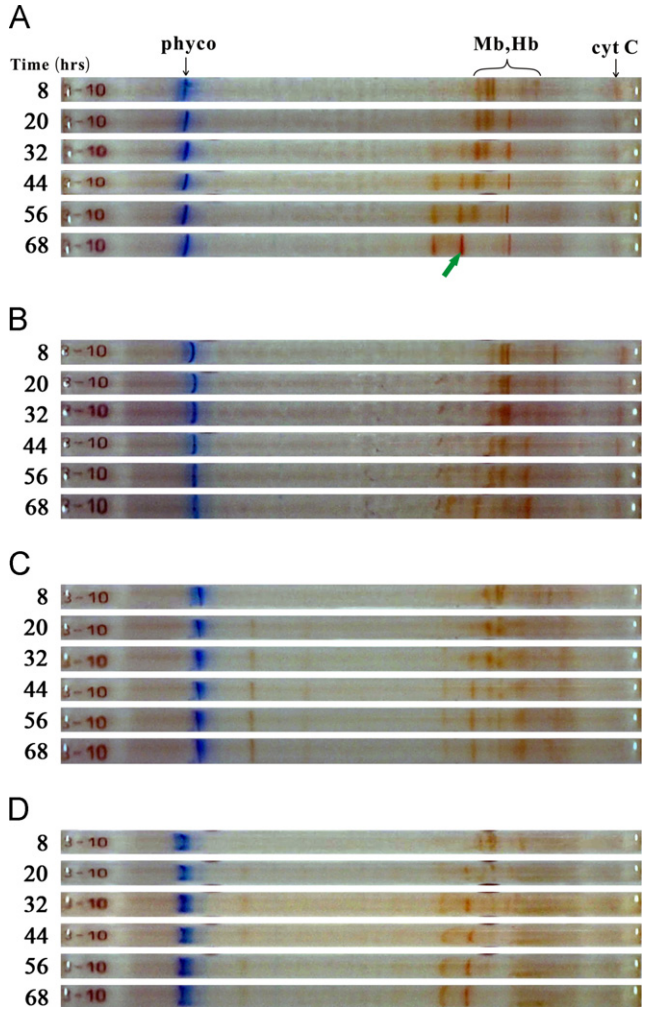

Fig. 5. Electrophoregrams of standard proteins focused in IPG–IEF with salt mobilization under the conditions of (A) 80 mM H_2SO_4+50 mM Na_2SO_4 as the anolyte and 200 mM NaOH as the catholyte; (B) 80 mM H_2SO_4+100 mM Na_2SO_4 as the anolyte and 200 mM NaOH as the catholyte; (C) 80 mM H_2SO_4+150 mM Na_2SO_4 and 200 mM NaOH; and (D) 80 mM H_2SO_4+200 mM Na_2SO_4 and 200 mM NaOH. The other conditions are the same as those in Fig. 2. (Phyco: phycocinin, Mb: equine myoglobin, Hb: human hemoglobin, cyt C: cytochrome C). (For interpretation of the references to color in this figure, the reader is referred to the web version of this article.)

Figs. 5 and 6 exhibit the mobilization results of IPG–IEF run with the electrolyte pairs in Tables 1 and 2, respectively. As showed in Fig. 5, the anodic mobilization of pH gradient was initiated due to the addition of sodium sulfate in the anolyte. Panels A, B, C and D revealed the results with 50 mM, 100 mM, 150 mM, 200 mM Na_2SO_4, respectively. We could observe that the brown bands gradually drifted toward the anode in 8–68 h of IEF run and the drifting distance gradually increased as added salt concentrate enchanced. Even in Panels C and D, the brown bands drifted to the position near blue phycocynin and the intensity of the brown band near blue band gradually increased from 8 h to 68 h. Meanwhile, the intensity of the brown bands near the cathode gradually decreased. In all panels, the band of cytochrome C drifted toward the anode step by step and its intensity also decreased gradually from 8 h to 68 h. As shown in 68 h panel of Fig. 5A, the red band catch up with brown band and overlays with brown band (green arrow). It could be seen in Fig. 5A–D that pH gradient shifted faster toward the anode as R_r value increased.

Fig. 6 shows that mobilizations of IPG–IEF with 80 mM H_2SO_4 and 200 mM NaOH+50 mM, 100 mM, 150 mM, 200 mM Na_2SO_4 as the anolyte and the catholyte respectively. We could observe that the blue phycocynin band evidently drifted toward the cathode and the drifting distance gradually increased while the added salt concentrate increased. The blue band has an obvious drifting at

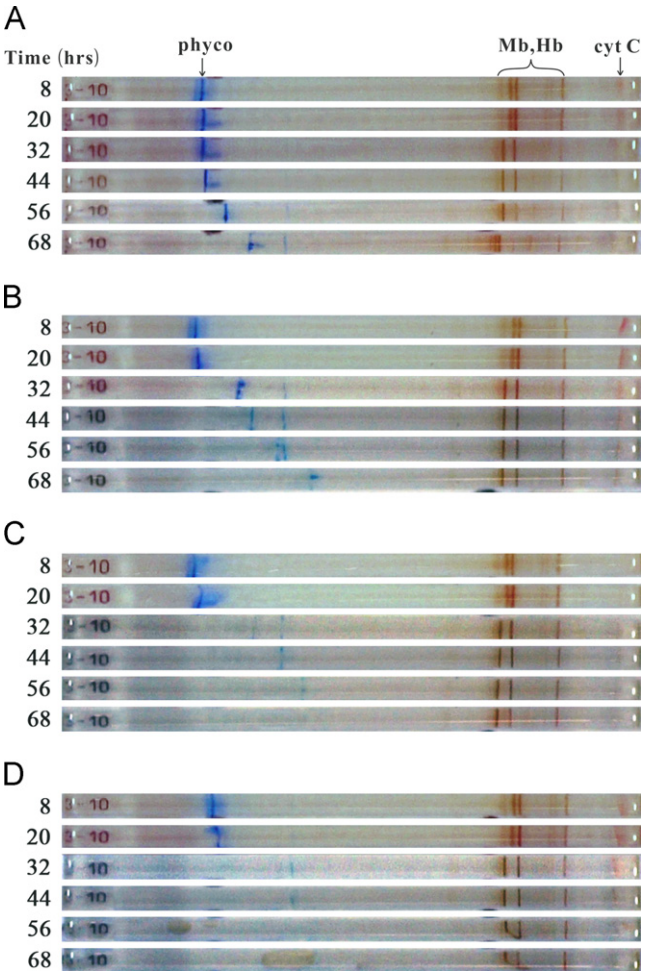

Fig. 6. Electrophoregrams of standard proteins focused in IPG–IEF with salt mobilization under the conditions of (A) 80 mM H_2SO_4 as the anolyte and 200 mM NaOH+50 mM Na_2SO_4 as the catholyte; (B) 80 mM H_2SO_4 and 200 mM NaOH+100 mM Na_2SO_4; (C) 80 mM H_2SO_4 and 200 mM NaOH+150 mM Na_2SO_4; and (D) 80 mM H_2SO_4 and 200 mM NaOH+200 mM Na_2SO_4. The other conditions were the same as those in Fig. 2. (Phyco: phycocinin, Mb: equine myoglobin, Hb: human hemoglobin, cyt C: cytochrome C).

56 h in Fig. 6A. However the obvious drifting appears at 32 h in Fig. 6B. There is farther drifting of blue band at 32 h in Panels C and D. Due to the red cytochrome C drifts to the cathode, we can observe that the intensity of the red band gradually decreases as the run prolonged at each panel in Fig. 6. Interestingly, the red bands firstly drifted toward the anode when salting in the anolyte and the blue protein firstly drifted toward the cathode when salting in the catholyte. This was presumably caused by heterogeneous salt concentrate distribution in IPG–IEF run.

Through the experiments above, one can conclud that pH gradient in an IPG–IEF run could be controlled by the fluxes of hydrogen and hydroxyl, viz., the R_r value of Eq. (4a). When $R_r > 0$, pH gradient drifted toward the cathode (Table 2), conversely toward the anode (Table 1). The higher R_r value was, the more serious the drifting became (Tables 1 and 2). These conclusions are in complete agreement with the theoretical results in Section 3.1, further testifying the validity of Eqs. (4a) and (4b) for IPG–IEF.

3.2.4. *Mechanism of weak pH gradient plateau in IPG–IEF*

The water production in IEF has a key role in the pH gradient plateau [29,30,35–38]. Theoretically, the more the water production is, the more obvious the pH gradient plateau is. Eqs. (16) and (17) further imply that the higher the current at steady-state of IEF is, the more water production turns, of course the more serious the pH gradient plateau in IEF is. From the comparison between Eqs. (13) and (14) or Eqs. (16) and (17), we could obtain the following predictions.

Prediction (**i**): the electric current of steady-state in IPG–IEF run ($I_{T,SS,IPG}$) is certainly less than that in non-IPG–IEF run ($I_{T,SS,non\text{-}IPG}$) due to much higher diffusional current of CA existing in non-IPG–IEF rather than IPG–IEF.
Prediction (**ii**): the pH gradient plateau in IPG–IEF is necessarily weaker than that in non-IPG–IEF due to the existence of $I_{T,SS,IPG} < I_{T,SS,non\text{-}IPG}$, viz., Prediction (1).
Prediction (**iii**): the comparison of Eqs. (13) and (14) indicates that the electromigration current at initial stage of IPG–IEF ($I_{EMC,IPG}$) is clearly lower than that of non-IPG–IEF due to more free CA species used in non-IPG–IEF but not in IPG–IEF.

Prediction (**i**) was manifested by the following experiments on current comparison between IPG–IEF and non-IPG–IEF runs. Fig. 7 shows the curve of current versus run-time in both IPG–IEF and non-IPG–IEF. Note here, there was a slight difference of voltage used in IPG–IEF and non-IPG–IEF. For the convenient comparison from the beginning to the end, the current value in Fig. 7 is transferred as the one at unit voltage used in the two IEF runs. In Fig. 7A, the current decreases from the maximum value of 1 μA/V to 0.1 μA/V within 200 min run, and around 0.07 μA/V at the end of IEF. In the run of non-IPG–IEF in Fig. 7B, the current reduced from the maximum (37 μA/V) to 1.0 μA/V within about 300 min run, and further declined to around 0.5 μA/V until the end of non-IPG–IEF. The comparison of steady-state current in Fig. 7A and B evidently demonstrates **Prediction** (**i**).

Obviously, **Prediction** (**ii**) was demonstrated by the experimental results in Fig. 7 and the comparative experiments of both Fig. 2 (the weak pH gradient plateau in IPG–IEF) and Fig. 3 (the obvious plateau in non-IPG–IEF). And the comparison of electromigration current within 150 min run in Fig. 7A and 200 min run in Fig. 7B clearly manifestes the validity of **Prediction** (**iii**).

It was observed that the electromigration current at the initial stage of non-IPG–IEF was greatly higher than that of IPG–IEF. This might be caused by the following reasons. First, the quantity of CAs (2%) used in non-IPG–IEF was clearly higher than that (0.5%) used in IPG–IEF. Second, a certain quantity of inorganic salt (ammonium sulfate 0.06%) was present in non-IPG–IEF, which had a contribution to the electromigration current.

4. Conclusions

In this study, we developed the theories on the judgment expression in IPG–IEF system, the current formation (especially the diffusional current) and the water production in the IEF system and deduced relevant equations which could well predict the stability of pH gradient in IEF. Two novel techniques of IEF were developed, including mobilization of pH gradient in IPG–IEF and non-IPG–IEF with IPG–IEF focusing tray. Subsequently stability mechanism of IPG–IEF was explored by the theories and a series of experiments. It was revealed that (i) there existed high diffusional current in non-IPG–IEF due to the diffusion of free CAs, resulting in more water production and more distinct plateau phenomenon, (ii) there was almost no diffusional current in the IPG–IEF due to the immobilization of CAs in gel matrix, leading to less water products and slight plateau phenomenon, (iii) the pH gradient drifting could be effectively controlled by IPG technique due to the equal-fluxes of hydroxyl and hydrogen ions in the IPG–IEF system, and (iv) an immobilized pH gradient could be mobilized by salting into either anolyte or catholyte to change the fluxes of hydroxyl and hydrogen ions in the developed IPG–IEF system.

Acknowledgments

We thank the NSFC (No. 21035004), the National Key Program of Scientific Instrument of China (No. 2011YQ030139), National Basic Research Program of China (973 Program, No. 2009CB118906) and

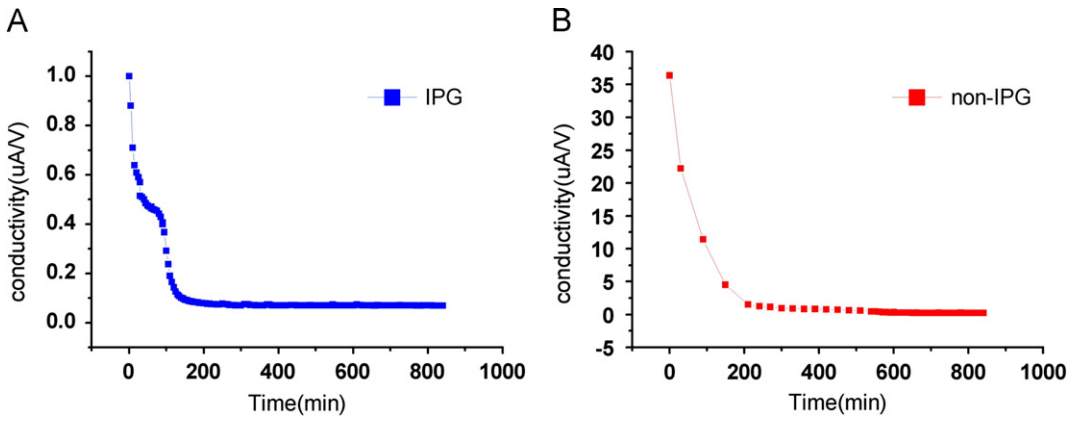

Fig. 7. Curves of the current versus the run-time in (A) IPG–IEF and (B) non-IPG–IEF. The conditions of Panels A and B are the same as those in Figs. 2 and 3, respectively.

the Shanghai Jiao Tong University (No. YG2010ZD209) for financial support of this research.

Appendix A. Supporting information

Supplementary data associated with this article can be found in the online version at http://dx.doi.org/10.1016/j.talanta.2013.03.026.

References

[1] P.G. Rightti, in: T.S. Work, R.H. Rurdon (Eds.), Laboraotary Techniques in Biochemistry and Molecular Biology, vol. II, Elsevier Biomedical Press, Amesterdam, New York, Oxford, 1983, pp. 1–86 268–313.
[2] H. Svensson, Acta Chem. Scand. 15 (1961) 325.
[3] H. Svensson, Acta Chem. Scand. 16 (1962) 456.
[4] A. Carlstrom, O. Vesterberg, Acta Chem. Scand. 21 (1967) 271.
[5] O. Vesterberg, Acta Chem. Scand. 23 (1969) 2653.
[6] P.H. O'Farrell, J. Biol. Chem. 250 (1975) 4007.
[7] Nilesh S. Tannu, Scott E. Hemby, Nat. Protocols 1 (2006) 1732.
[8] A.D. Rolland, B. Evrard, N. Guitton, J. Proteome Res. 6 (2007) 683.
[9] G.R. Finlayson, A. Chrambach, Anal. Biochem. 40 (1971) 292.
[10] L.E.M. Miles, G.E. Simmons, A. Chrambach, Anal. Biochem. 49 (1972) 109.
[11] N.Y. Nguyen, A. Chrambach, Anal. Biochem. 82 (1977) 226.
[12] N.Y. Nguyen, A.G. McCormick, A. Chrambach, Anal. Biochem. 88 (1978) 186.
[13] Z. Buzas, L.M. Hjelmeland, A. Chrambach, Electrophoresis 4 (1983) 27.
[14] G. Baumann, A. Chrambach, Progress in Islelectric Focusing and Isotachophoresis, in: P.G. Righetti (Ed.), North-Holland Publishing Co., Amsterdam, 1975, p. 13.
[15] H. Rilbe, Electrofocusing and Isotachophoresis, in: B.J. Radola, D. Graeslin (Eds.), Walter de Gruyter & Co., Berlin, New York, 1977, p. 35.
[16] L.E.M. Miles, G.E. Simmons, A. Chrambach, Anal. Biochem. 49 (1972) 109.
[17] S. Pollack, Biochem. Biophys. Res. Commun. 87 (1979) 1252.
[18] J. Deman, W. Rigole, J. Phys. Chem. 74 (1970) 1122.
[19] B. Bjellqvist, K. Ek, P.G. Righetti, E. Gianazza, A. Görg, R. Westermeier, W. Postel, J. Biochem. Biophys. Methods 6 (1982) 317.
[20] P.G. Righetti, E. Gianazza, B. Bjellqvist, K. Ek, A. Görg, R. Westermeier, in: D. Stathakos (Ed.), Electrophoresis '82, de Gruyter, Berlin, 1983, p. 75.
[21] B. Bjellqvist, K. Ek, P.G. Righetti, E. Gianazza, A. Görg, W. Postel, Prot. Biol. Fluids 30 (1983) 599.
[22] W. Görg, R. Postel, B. Westermeier, K. Bjellqvist, E. Ek, P.G. Gianazza, Prot. Righetti, Biol. Fluids 30 (1983) 607.
[23] A. Görg, W. Postel, R. Westermeier, B. Bjellqvist, K. Ek, E. Gianazza, P.G. Righetti, in: D. Stathakos (Ed.), Electrophoresis '82, de Gruyter, Berlin, 1983, p. 353.
[24] A. Görg, W. Postel, R. Westermeier, B. Bjellqvist, K. Ek, E. Gianazza, P.G. Righetti, Prot. Biol. Fluids 30 (1983) 607.
[25] T.T. Wang, J.F. Ma, G.J. Zhu, J. Sep. Sci. 33 (2010) 3194.
[26] Z.C. Zhang, J.H. Wang, L.M. Hui, Electrophoresis 33 (2012) 661.
[27] Y. Liang, Y.Z. Cong, Z. Liang, Electrophoresis 30 (2009) 4034.
[28] M. Pernemalm, J. Lehtio, J. Proteome Res. 12 (2013) 1014.
[29] C.X. Cao, J. Chromatogr. A 813 (1998) 153.
[30] C.X. Cao, L.Y. Fan, W. Zhang, Analyst 133 (2008) 1139.
[31] J. Deman, W. Rigole, J. Phys. Chem. 74 (1970) 1122.
[32] J. Deman, Anal. Chem. 42 (1970) 321.
[33] J. Pospichal, M. Deml, P. Gebauer, P. Bocek, J. Chromatogr. 470 (1989) 43.
[34] J. Pospichal, M. Deml, P. Bocek, J. Chromatogr. 638 (1993) 179.
[35] H. Liang, Y. Chen, L.J. Tian, L. Zhang, Electrophoresis 30 (2009) 3134.
[36] H. Liang, L.F. OuYang, Q. Liu, L. Zhang, L.J. Tian, Y. Chen, J. Sep. Sci. 34 (2011) 1212.
[37] C.-X. Cao, J. Chromatogr. A 813 (1998) 173.
[38] Y.J. Xu, S. Li, W. Zhang, L.Y. Fan, J. Shao, C.X. Cao, J. Sep. Sci. 32 (2009) 585.
[39] S. Li, C.-X. Cao, Z.-X. Lin, J.-F. Luo, Colloid. Polym. Sci. 283 (2005) 1131.
[40] W.T. Moore, Physics Chemistry, 6th Ed., Longman Group Ltd., London, 1976, p. 435.
[41] W. Adamson, A Textbook of Physical Chemistry, Acadimic Press, London, 1973, p. 486.